Proceedings of the International Conference "Underwater Acoustic Measurements: Technologies & Results"
Heraklion, Crete, Greece, 28th June – 1st July 2005

THE SOUNDS OF SEAS IN SPACE

Timothy G. Leighton, Paul R. White & Daniel C. Finfer

Institute of Sound and Vibration Research, Southampton University, Highfield, Southampton, SO17 1BJ, United Kingdom.

Professor Timothy G. Leighton, Institute of Sound and Vibration Research, Southampton University, Highfield, Southampton, SO17 1BJ, United Kingdom. Fax: 44 (0)2380 593190; tgl@soton.ac.uk

Abstract: *On 14 January 2005 the Huygens space probe landed on Titan, the surface of which had previously been obscured by smog. This exercise was undertaken prior to the probe's successful landing, in an attempt to calculate the sounds which would be associated with splashdowns and methane-falls, in the hypothetical scenario that (of the many sensing systems on Huygens) only the acoustic information was available in order to interpret conditions on Titan. The exercise includes innovations in the inversion of bubble entrainment noise to estimate bubble populations, and illustrates the benefits of using acoustics for space exploration.*

Keywords: *Ambient noise, Titan, entrainment, passive, waterfall*

1. INTRODUCTION

After a 7-year journey on NASA's *Cassini* spacecraft, the European Space Agency's *Huygens* probe landed on Saturn's largest moon, Titan, on January 14. It takes a moment to understand the step-change in knowledge that took place on that day. The surface of the planet is obscured with smog, and while we could envisage the possibility of seas, waves and waterfalls, and the equivalent of Earth's water cycle based on liquid methane and ethane, when the investigation of this paper began, we had no sure knowledge that these existed [1-3]. *Huygens* was ingeniously designed to cope with a range of terrains, from liquid to solid, and this investigation addressed two possibilities: if the descent had ended with a splashdown

in liquid; or (perhaps less likely) if the landing site had been close to a methane-fall. The characteristics of acoustic sensors tally well the constraints of space travel: acoustic instrumentation is low-cost, rugged and durable, has low power consumption, and generates signals of low bandwidth compared to the imaging systems more usually exploited off-world. Indeed, whilst eventually *Huygens* managed to transmit for several hours on the surface, many expected only 3 minutes of battery life would remain after landing. *Huygens* was designed with an acoustic capability [4].

Whilst it is recognised that acoustic technology could never replace imaging, the possibility was explored as to what could be gained were only the acoustic systems to be operational after landing: "If there is a splash and not a crunch when the probe lands, that would make Titan the first known body other than Earth to have an ocean open to an atmosphere. This would mean there could be babbling brooks and streams; and a beach at minus 180 degrees C" [5]. In the first stage [2], an appropriate model for the emission of bubbles was chosen and used to invert the sound of a terrestrial waterfall (the Salmon Leap, at Sadler's Mill, Romsey, Hampshire, UK). Such inversions are not uncommon. They range from the identification of individual bubble signatures with entrainments of bubbles of calculated sizes [6] (later augmented by use of the Gabor transform when entrainment rates or noise were high [7]), to the recreation of the overall power spectrum using the cumulative spectral content of naturally-emitting bubbles. The latter approach was pioneered by Loewen and Melville [8]. None of these models are entirely suitable (see section 2 and ref. [9]): the initial study [2] used a monopole version of the model of ref. [8], although with the heuristic approach to the amplitude of the bubble pulsations replaced by a physics-based one. The Salmon Leap bubble population was then used to estimate the sound that a methane-fall would make, if there were one on Titan which had the same entrainment statistics (not an unreasonable suggestion given the fluid parameters [2]). The reconstructed power spectrum for the terrestrial waterfall agreed with the measured Salmon Leap data, allowing some credibility to be given to the predicted spectrum for Titan. Recordings of these sounds, and similar predictions of possible splashdown sounds, can be accessed via the web page [10]. Nevertheless, the inversion was conducted without reference to the higher order moments [11], and the associated discrepancies were evident in listening-test comparisons of the measured and reconstructed Salmon Leap data. In addition, whilst the general shape of the predicted spectrum for Titan agreed with back-of-the-envelope calculations [2] and appeared to be physically sensible, the absolute spectral levels seemed to be too high. Therefore this study set out to provide a more stringent inversion routine. Furthermore, a very different waterfall was chosen in order to test the general trends found in the first study (Fig. 1).

2. THEORY

The method used to compute the bubble size distribution is an extension of the classical technique of Loewen and Melville [8]. This extension differs from the original approach in three ways: first a pair of measurements are exploited; second the contribution of each ringing bubble is not constrained to lie in a single frequency bin; third a monopole model for the bubbles is used because, despite the fact that the bubbles are entrained near the surface, the dipole model of Loewen and Melville is not suitable for our measurement geometry.

As with all acoustic inversion models one needs a forward model that predicts measurable acoustic quantities from physical parameters. There are several forward models that one might choose to exploit, depending upon the particular measurement geometry. Whilst the choice of model significantly affects the results one obtains from a particular data set, it is not fundamental to the principle described herein. Therefore we initially describe the technique in

the absence of specifics relating to the forward model, and only later provide the details of the exact model employed to obtain our results. Thus we denote our forward model as follows

$$p(t) = \Pi(t; t_0, r, h, R_0) = \Pi(t - t_0; r, h, R_0) \tag{1}$$

where $p(t)$ represents the measured pressure at the hydrophone, t_0 is the instant at which the pressure fluctuation from the bubble first arrives at the hydrophone, r is the range from hydrophone to the bubble, h is the entrainment depth, R_0 is the bubble's equilibrium radius and the function Π is simply a formal mechanism that relates the physical parameters to the measured time series. In the context of this paper, different forms of the function Π can be defined for Earth and Titan, which correspond to the differing environmental conditions.

The measured pressure at the hydrophone is simply the sum of the contributions from all the bubbles, so that

$$p_m(t) = \sum_{n=1}^{N} \Pi(t - t_{0,n}; r_n, h_n, R_{0,n}) \tag{2}$$

where the index n is included to indicate physical parameters of an individual bubble. If one assumes a spatially localised bubble cloud, characterised by a constant entrainment depth, then one can assume that r_n and h_n are independent of n; the notation r and h will be adopted for these fixed values. By using time-averaged quantities one is able to remove the temporal dependence in (2) and if these quantities obey a superposition principle then the structure of (2) remains unchanged. Specifically if the time-averaged operator is denoted $C\{\}$ then

$$\Omega = C\{p_m(t)\} = \sum_{n=1}^{N} C\{\Pi(t - t_{0,n}; r, h, R_{0,n})\} \tag{3}$$

in which the assumption of a superposition principle for $C\{\}$ has been exploited. The most obvious choice for a general class of operators $C\{\}$ are temporal estimates of cumulants [12]. The second order cumulant relates directly to power. It should be noted that the superposition principle for cumulants requires that the bubble signatures are statistically independent. Whilst the second order cumulant is the obvious choice for this operator, the advantages of using higher order cumulants has been highlighted elsewhere [13]. In order to obtain a tractable solution based on (3) it is necessary to approximate the summation over all bubbles by a radius binned form, namely:

$$\Omega \approx \sum_{i=1}^{B} N(R_i)\chi(R_i, h, r) \qquad \chi(R_i, h, r) = \overline{C\{\Pi(t - t_0; h, r, R_0)\}}. \tag{4}$$

The over-bar notation indicates that an average has been conducted over the values of R_0 in the i^{th} bin, R_i is the centre radius in the i^{th} bin, $N(R_i)$ is the number of bubbles in the radius bin and B is the number of bins. If the chosen operator is the second order cumulant (power) then χ is reflects the average power of a bubble in a particular radius bin. The inversion method used by Loewen and Melville was simplified by use of the assumption that all of the energy contributed by bubbles in a given radius bin occur at a particular frequency (the natural frequency of a bubble of radius R_i). Application of this assumption allows one to write:

$$\Omega(f_k) \approx N(R_i)\chi(R_i, h, r) \tag{5}$$

where $\Omega(f_k)$ is the value of $C\{p_m(t)\}$ once $p_m(t)$ has been band-pass filtered about f_k. Since values of χ can be readily estimated from the model, then (5) allows estimation of the number

of bubbles. To obtain (5) one assumes that a given bubble only contributes to one frequency bin. This assumption is only reasonable if wide frequency bins are employed, specifically if the frequency bin width is significantly larger than the bandwidth of the bubble signature. As a result, this approximation provides a lower limit on the realisable resolution of the method. An alternative approach is to account for the contributions of bubbles in all frequency bins, so that (5) becomes

$$\Omega(f_k) = \sum_{i=1}^{B} N(R_i)\tilde{\chi}(R_i, f_k) \tag{6}$$

in which $\tilde{\chi}(R_i, f_k)$ represents the contribution of bubbles in the i^{th} radius bin to the k^{th} frequency bin. One can employ equal numbers of frequency and radius bins, most conveniently arranged so that the frequencies map to the resonant frequencies of the bubbles with the specified radii. In such circumstances (6) represents a linear system of equations which can be solved using standard matrix methods. The reader is reminded that (6) is general in the sense that it applies to any operator $C\{\}$ with the stated properties.

When using the second order cumulant (which relates to power) then background noise can represent a significant problem. Specifically the value of $\Omega(f_k)$ is the addition of the power of the bubbles signatures and the noise, leading to an overestimation of the number of bubbles. In the experiment presented here, we are able to mitigate against this by placing a hydrophone some distance from the localised source of bubble noise, allowing us to make an independent measurement of the background noise. This noise contains some contribution from the bubbles, an effect that can be further mitigated by replacing the temporal average used when computing $\Omega(f_k)$ with a temporal median. The median removes outlying values and can be corrected to provide a robust estimate of the mean [14]. This will be denoted $\Omega_{noise}(f_k)$. Thus our power-based estimate of the bubble population is obtained, in matrix form, as

$$\underline{N} = \tilde{\boldsymbol{\chi}}^{-1} \max\left\{\underline{\Omega} - \underline{\Omega}_{noise}, 0\right\} \tag{7}$$

where $\underline{N}$, $\underline{\Omega}$ and $\underline{\Omega}_{noise}$ are $B\times1$ column vectors and $\tilde{\boldsymbol{\chi}}$ is a matrix of values of $\tilde{\chi}(R_i, f_k)$. Inverses based on (7) rely on the numerical qualities of the matix $\tilde{\boldsymbol{\chi}}$. If the condition number in the matrix is large then the inversion will be sensitive to noise. In the passive inversion problem the conditioning of this matrix is not a fundamental problem, because the matrix has does not have large off-diagonal terms. This is in contrast to inversions based on active bubble sizing problems where the matrix inversion is hindered by ill-conditioning [15]. The condition number of the matrix $\tilde{\boldsymbol{\chi}}$ only becomes problematic when small bin sizes are used. By suitable bin size selection one can avoid the need for regularisation. This is a fundamental restriction on bin sizes which is less stringent than that imposed by the assumption inherent in (5).

Having obtained a bubble population, the forward model (2) can then be used to synthesize time series for the bubble entrainment noise. To synthesize a measured hydrophone signal, one should also create a background noise signal with the characteristics of $\Omega_{noise}(f_k)$, which can be realised by filtering Gaussian white noise. To synthesize the noise of bubbles being entrained under different physical conditions, one simply needs to substitute the appropriate function Π during the synthesis process, i.e. implementation of (2).

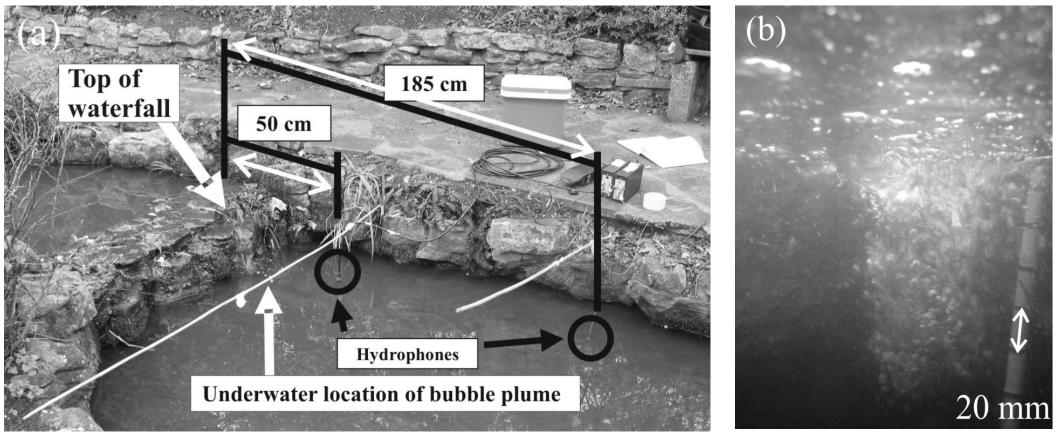

Fig. 1: (a) Equipment layout during data capture in the creek on the Highfield Campus (University of Southampton). Vertical arrow shows location of bubble entrainment photographed underwater in (b), where the scale bar is based on not-quite vertical measuring pole.

3. EXPERIMENT

The data for our experiments were collect from a small waterfall on the Highfield campus of the University of Southampton, Southampton UK. The waterfall is one of several in a series along a creek passing through the centre of the campus, and is pictured in Fig. 1(a). Two hydrophones were used to make acoustic observations: a Reson NUMBER (S/N 1999014) and a Bruel and Kjaer 8104 (S/N 2262868). Bruel and Kjaer Type 2635 charge amplifiers were used to deliver the signal to a 2-channel battery-powered Aiwa HHB 1 Pro DAT recorder recording at 44.1 kHz per channel. Anti-aliasing filters are incorporated into the DAT recorder device. DAT analogue output was captured to computer using an Edirol UA-1A USB audio interface using Adobe Audition.

The acoustic centre of each hydrophone was 10 cm beneath the surface, with the closest sensor being approximately 50 cm from the waterfall and the second senor being 1.85 m. Recordings were made covering two configurations, with the positions of the two sensors being reversed. Underwater photos were taken to allow estimates of bubble entrainment depth to be formed. One such photo is shown in Fig. 1(b).

4. RESULTS

The data corresponding to recordings made using the same hydrophone at the two locations were analysed. Fig. 2 illustrates the power spectra computed in these locations. In the distance location median processing has been used to attenuate further the effect of the waterfall and to provide an improved estimate of the background noise. These spectra demonstrate that there dominant frequency band containing bubble entrainment noise is roughly 1-10kHz. Below 1 kHz the first order assumption is made that the signal is dominated by hydrodynamic noise from the waterfall (this can be tested using the fact that hydrodynamic signals attenuate at different rates to acoustic ones); and above 10 kHz the spectra are dominated by a non-bubble noise (characterised as such because of its similarity at both hydrophones). An inversion based on (7) was performed; using 5, 10, 15 and 20 radius bins in the frequency range 1-10 kHz. The results are shown in Fig. 3 expressed in

number of bubbles entrained per micrometer radius increment per second. The bubble distributions estimated in this manner show considerable consistency. The case where 20 radius bins are employed does show an oscillatory behaviour and does generate a negative bubble populations for one bin, highlighting the fact that for this choice of bin size the $\tilde{\chi}$ matrix is becoming ill-conditioned.

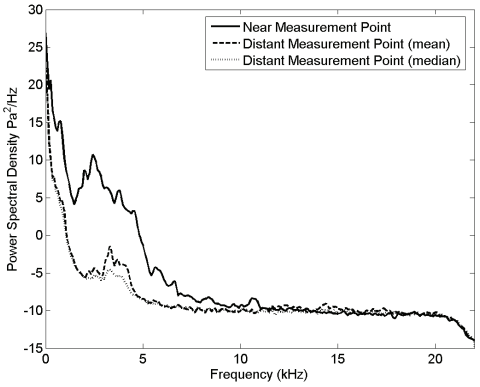

Fig. 2: Power spectra computed from data measured at two locations shown in Fig. 1, expressed in dB.

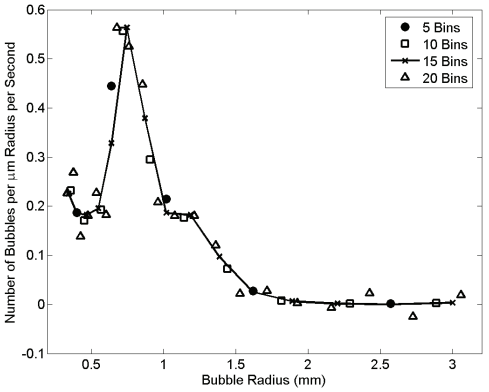

Fig. 3: Inversions results for different numbers of size bins.

Data from this inversion were then used to synthesize the original recordings and so produce a test dataset that can be used for algorithmic validation. Fig. 4 shows four sets of results, those for an inversion based on (7), that are based on acoustic power, and results based on (6) in which the fourth order cumulant has been used. Since the fourth order cumulant is unaffected by additive Gaussian noise then there is no need to form a separate estimate of the background noise contribution, so (6) can be solved directly. For the synthetic data the fourth order inversion agrees with results for the power based method (using the measured and synthetic data sets). However the inversion for the fourth order scheme provides a large overestimate of the bubble population when applied to the measured data. These results are consistent for different bins sizes (results not shown here), demonstrating that this is not a consequence of ill-conditioning. The fact that the fourth order inversion scheme functions correctly on the synthesised data provides confidence that it is algorithmically correct. This leads one to suggest that the model on which the method is based is in some sense incomplete. Listening to the synthesised data provides further evidence for this. The synthetic and measured data have the same power spectrum (which is a necessary condition for the inversion from the synthetic data to match the results from the measured data, see Fig. 4). Despite this spectral equivalence the subjective quality of the synthetic signal is quite different to the measured signal as was observed for the data from Salmon Leap [2].

Fig. 5 shows the power spectral densities computed using the data obtained by inverting bubble size distributions measured on Earth; but during the inversion the environmental parameters for Titan are employed. Thus one obtains a prediction for the sound of a methane-fall on Titan. It can be seen from Fig. 5 that the general effect is to shift the spectrum upwards in frequency, creating a higher pitched sound, confirming the trend of [2]. However this improved method removes the high spectral levels judged to be unreliable in the predictions of [2], and shows a more physically realistic reduction in the overall signal power (~17 dB).

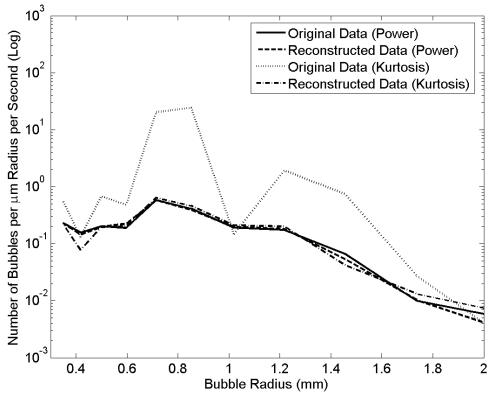

Fig. 4: Estimated bubble populations.

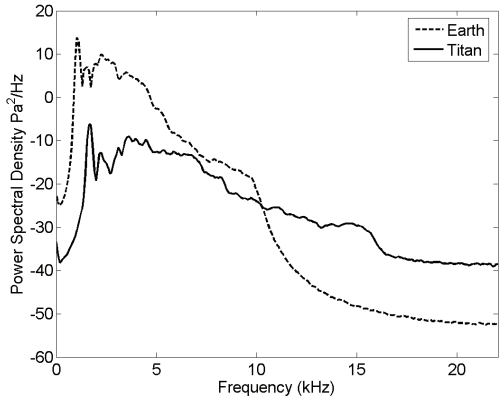

Fig. 5: Power spectral densities for bubble entrainment noise, expressed in dB.

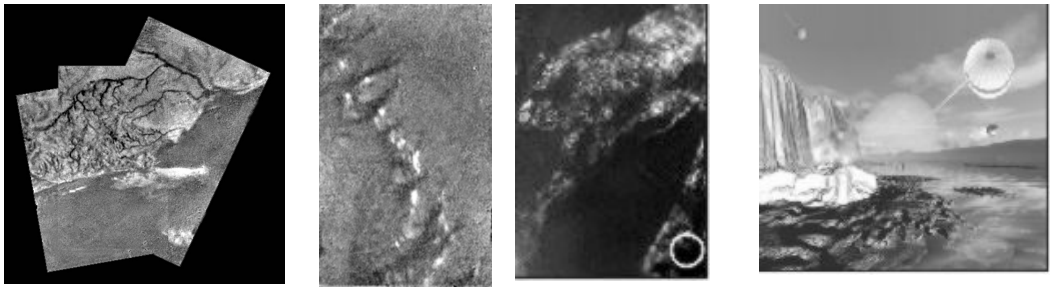

(a) *(b)* *(c)* *(d)*

Fig. 6: Images of Titan obtained by the Huygens probe. (a) This mosaic of three frames provides detail of a high ridge area including the flow down into a major river channel from different sources. (b) A single image from the Huygens DISR instrument of a dark plain area on Titan, seen during descent to the landing site. There appears to be flow around bright 'islands'. The areas below and above the bright islands may be at different elevations. (c) The landing site of Huygens is circled. (d) Impression by artist (David Seal) of Titan's surface. Cassini flies over the surface as the Huygens probe nears the end of its parachute descent. Thin methane clouds dot the horizon, and a narrow methane spring or "methane-fall" flows from the cliff at left. Smooth ice features rise out of the methane/ethane lake. (Credits: ESA/NASA/JPL/University of Arizona)

5. CONCLUSIONS

This paper has outlined an advance on the existing techniques for inverting the entrainment emissions of bubbles, and applied it to estimate the sounds of methane-falls on Titan. Whereas the initial study [2] estimated spectral levels on Titan that were ~10 dB greater than the terrestrial values, refinement of the assumptions associated with the excitation predicts similar levels for the two (Fig. 5). The general shift in energy to higher frequencies is very similar in both studies, and to be expected from back-of-the-envelope calculations [2]. In its descent, *Huygens* photographed features which are currently believed to reflect the presence of flowing liquid on Titan (Fig. 6(a),(b)), which carves out valleys and presumably is likely to generate methane-falls. The landing site, though possibly close to such an area (Fig. 6(c)), is thought to be on a mud- or snow-like surface, and hence the

microphone on the probe did not detect the sound of either a splashdown or a methane-fall. Such a methane-fall is depicted in Fig. 6(d), falling into a crater sea on Titan. Sounds of splashdowns and methane-falls are available at the website [8].

The purpose of this exercise is to demonstrate the opportunities which acoustic measurements offer for space exploration. The signal has low bandwidth, the hardware is rugged, and typically has low mass, low cost, and low power requirements. Given the myriad uses for diagnosis by bubble-generated sound on Earth, from rainfall sensing to investigating atmosphere/ocean mass flux, this exercise illustrates that the use of sound in general as an extraterrestrial diagnostic presents intriguing possibilities.

REFERENCES

[1] **Ghafoor, N.A.-L., Zarnecki, J.C., Challenor, P.G.** and **Srokosz, M.A.**, Wind-Driven Surface Waves On Titan. *J. Geophys. Res.* **105**(E5), 12077-12091, 2000.

[2] **Leighton, T.G.** and **White, P.R.**, The sound of Titan: a role for acoustics in space exploration. *Acoustics Bulletin* **29**, 16-23, 2004.

[3] **Leighton, T.G.**, From seas to surgeries, from babbling brooks to baby scans: The acoustics of gas bubbles in liquids', *International Journal of Modern Physics B,* **18**(25), 3267-3314, 2004.

[4] **Svedhem, H., Lebreton, J.-P., Zarnecki, J.** and **Hathi, B.**, Using Speed of Sound Measurements to Constrain the Huygens Probe Descent Profile. In: Wilson, A. (Ed.), *Proc. Int. Workshop on Planetary Probe Atmospheric Entry and Descent Trajectory Analysis and Science,* Lisbon, 6-9 October 2003. ESA SP-544, pp. 221-228, 2004.

[5] **Leighton, T.G.**, BBC News Online, July 1, 2004.

[6] **Leighton, T.G.** and **Walton A.J.**, An experimental study of the sound emitted from gas bubbles in a liquid, *European Journal of Physics*, **8**, 98-104, (1987).

[7] **Leighton, T.G, White, P.R.** and **Schneider, M.F.**, The detection and dimension of bubble entrainment and comminution, *Journal of the Acoustical Society of America*, **103**(4), 1825-1835, 1998.

[8] **Loewen, M.R.** and **Melville, W.K.**, A model for the sound generated by breaking waves. *J. Acoust. Soc. Am.* **90**, 2075-2080, 1991.

[9] **Leighton, T.G.**, *Bubble Acoustics from Seas to Surgeries*. Springer Series in Modern Acoustics and Signal Processing series, Springer, 2005 (in preparation).

[10] **Leighton, T.G.**, www.isvr.soton.,ac.uk/fdag/uaua.htm, 2004.

[11] **Leighton T.G., White P.R.** and **Finfer D.C.**, Possible applications of bubble acoustics in Nature. *Proc. of the 28th Scandinavian Symposium on Physical Acoustics* (Ustaoset, Norway, 2005) (in press).

[12] **Mendel J.M.**, Tutorial on higher-order statistics in signal processing and system theory: theoretical results and some applications; *Proc. IEEE*, 79, 278-305 (1991).

[13] **White P.R.**, **Leighton T.G.** and **Yim G.T.**, Exploitation of higher order statistics to compute bubble cloud densities; evading Olber's paradox, *Proc. 7th European Conf. on Underwater Acoustics*, 223-228 (2004)

[14] **Leung T.S-T.** and **White P.R.**, Robust Estimation of Oceanic Background Noise Spectrum *Proc. 4th IMA Int. Conf. on Mathematics in Signal Processing*, Warwick, *unpaginated*, 1996

[15] **Leighton T.G., Meers S.D.** and **White P.R.**, Propagation through nonlinear time-dependent bubble clouds, and the estimation of bubble populations from measured acoustic characteristics. *Proceedings of the Royal Society A,* **460**(2049), 2521-2550, 2004.